Published in final edited form as:
Pharm Res. 2013 September ; 30(9): 2279–2289. doi:10.1007/s11095-013-1139-8.

Role of Intracellular Calcium in Proteasome Inhibitor-induced Endoplasmic Reticulum Stress, Autophagy and Cell Death

Jessica A. Williams[1,#], **Yifeng Hou**[2,#], **Hong-Min Ni**[1], and **Wen-Xing Ding**[1,*]

[1]Department of Pharmacology, Toxicology and Therapeutics, The University of Kansas Medical Center, Kansas City, KS

[2]Department of Breast Surgery, Breast Cancer Institute, Cancer Hospital, Fudan University, Shanghai, China

Abstract

Purpose—Proteasome inhibition induces endoplasmic reticulum (ER) stress and compensatory autophagy to relieve ER stress. Disturbance of intracellular calcium homeostasis can lead to ER stress and alter the autophagy process. It has been suggested that inhibition of the proteasome disrupts intracellular calcium homeostasis. However, it is unknown if intracellular calcium affects proteasome inhibitor-induced ER stress and autophagy.

Methods—Human colon cancer HCT116 Bax positive and negative cell lines were treated with MG132, a proteasome inhibitor. BAPTA-AM, a cell permeable free calcium chelator, was used to modulate intracellular calcium levels. Autophagy and cell death were determined by fluorescence microscopy and immunoblot analysis.

Results—MG132 increased intracellular calcium levels in HCT116 cells, which was suppressed by BAPTA-AM. MG132 suppressed proteasome activity independent of Bax and intracellular calcium levels in HCT116 cells. BAPTA-AM inhibited MG132-induced cellular vacuolization and ER stress, but not apoptosis. MG132 induced autophagy with normal autophagosome-lysosome fusion. BAPTA-AM seemed not to affect autophagosome-lysosome fusion in MG132-treated cells but further enhanced MG132-induced LC3-II levels and GFP-LC3 puncta formation, which was likely via impaired lysosome function.

Conclusions—Blocking intracellular calcium by BAPTA-AM relieved MG132-induced ER stress, but it was unable to rescue MG132-induced apoptosis, which was likely due to impaired autophagic degradation.

Keywords

Proteasome Inhibitor; ER stress; Autophagy; Intracellular Calcium; Cell Death

INTRODUCTION

There are two major cellular degradation systems in mammalian cells: the ubiquitin-proteasome system (UPS) and macroautophagy, which is later referred to as autophagy. The UPS is a major degradation system for short-lived proteins that are labeled with ubiquitin (1). Three types of enzymes, E1, E2 and E3, carry out protein-ubiquitin reactions in which

Correspondence should be addressed to: Wen-Xing Ding, Ph.D., Department of Pharmacology, Toxicology and Therapeutics; The University of Kansas Medical Center; MS 1018 3901, Rainbow Blvd.; Kansas City, Kansas 66160; Phone: 913-588-9813;Fax: 913-588-7501; wxding@kumc.edu.
[#]These two authors contribute equally to this work.

E1 activates ubiquitin, E2 transfers ubiquitin and E3 specifically targets ubiquitin to a specific protein. Subsequently, a fraction of proteins are specifically targeted and degraded by the 26S proteasome complex. Many critical proteins regulating cell proliferation and cell death need to be precisely regulated by the UPS. Therefore, suppression of the UPS with proteasome inhibitors, such as MG132, can induce both apoptotic and non-apoptotic cell death and has emerged as a new class of anticancer drug with great potential (2–5). For example, the proteasome inhibitor Velcade™ (Bortezomib) was approved by the FDA for treating refractory/relapsed multiple myeloma. However, resistance to proteasome inhibitors develops by unknown mechanisms (4).

Autophagy is another major intracellular degradation system. Unlike the UPS, autophagy is mainly responsible for the degradation of long-lived proteins and excess/or damaged organelles (6, 7). It is well known that autophagy is a cellular adaptive response to adverse conditions, such as in deprivation of nutrients or growth factors (8). Accumulating evidence supports that there is cross-talk between the UPS and autophagy. Inhibition of the proteasome has been shown to trigger autophagy, possibly as a compensatory mechanism, in many cell culture systems (9, 10). However, there was no difference in proteasome function between Atg7-deficient and wild type mouse brain tissue (11), suggesting that inhibition of autophagy does not necessarily lead to compensatory increased proteasome function. In contrast, inhibition of autophagy compromises UPS function due to excess p62 accumulation, which impairs the clearance of ubiquitinated proteins destined for proteasomal degradation (12).

Multiple mechanisms have been found to be important for proteasome inhibition-induced autophagy. We have previously demonstrated that proteasome inhibitors, such as MG132, induce autophagy in both cancer cells and non-transformed cells by triggering endoplasmic reticulum (ER) stress (9, 13). In response to ER stress, cells activate the unfolded protein response (UPR) as a protective and compensatory mechanism to relieve ER stress. Among the UPR signaling pathways, protein kinase RNA-like endoplasmic reticulum kinase (PERK) (14), eukaryotic translation initiation factor 2-alpha (elF2-alpha) (10), and inositol-requiring enzyme 1 (IREI)-mediated c-Jun N-terminal kinase (JNK) activation (9), have all been shown to be involved in proteasome inhibitor-induced autophagy. In all of these cases, it has been suggested that activated-autophagy serves as a cytoprotective mechanism to help remove misfolded proteins and protein aggregates caused by proteasome inhibition. Therefore, suppression of both the proteasome and autophagy has been shown to enhance proteasome inhibitor-induced cancer cell death (9, 10). Furthermore, the combination of proteasome and autophagy inhibitors, such as hydroxychloroquine, has been used in clinical trials as a novel strategy for enhanced cancer control (15).

Induction of ER stress can be triggered by disruption of intracellular calcium homeostasis, such as by treatment with thapsigargin, which inhibits the ER calcium-ATPase resulting in elevation of intracellular calcium (16). The role of calcium in autophagy is fairly complex and controversial. A rise in intracellular calcium levels, such as by vitamin D(3) compounds, ionomycin, ATP, and thapsigargin, induces autophagy by activating Ca(2+)/calmodulin-dependent kinase kinase-beta and AMP-activated protein kinase (17). Exogenous introduction of calcium by treating the cell with calcium phosphate precipitates (CPP) leads to a two-phase autophagic change: induction of autophagy at early time points (before 6 hours) followed by inhibition of autophagy at later time points (after 24 hours) due to impaired fusion of autophagosomes with lysosomes (18, 19). Furthermore, L-type calcium channel blockers also induce autophagy by inhibiting calpain activity, suggesting that cytosolic calcium may inhibit autophagy (20). It is well known that endosomes can fuse with lysosomes to form hybrid organelles in which the endocytosed cargo is degraded. It has been suggested that the fusion of autophagosomes with lysosomes could be similar to the fusion

of endosomes with lysosomes. Rab7, members of the HOPS complex, syntaxin 17, a hairpin-type tail-anchored SNARE protein (21), and lysosomal membrane proteins Lamp1 and Lamp2 have been implicated in the fusion of autophagosomes with lysosomes (22–24). Interestingly, it has also been suggested that calcium located within organelles is required for the fusion of late endosomes with lysosomes, a process which is inhibited by a cell permeable calcium chelator BAPTA-AM (1,2-bis-(o-aminophenoxy)-ethane-N,N,N',N'-tetraacetic acid, tetraacetoxymethyl esteris) (25). More recently, it was also suggested that thapsigargin can block the fusion of autophagosomes with lysosomes by altering cellular location of Rab7 (26). It has been shown that proteasome inhibition can alter intracellular calcium homeostasis (27), and we and others have demonstrated previously that proteasome inhibitors can induce autophagy in various cancer cell lines. However, it is not known if alteration of intracellular calcium affects proteasome inhibitor-induced ER stress and autophagy.

We report here that inhibition of the proteasome by MG132 induced elevation of intracellular calcium and ER stress. Blocking intracellular calcium with BAPTA-AM relieved MG132-induced ER stress, but it was not able to rescue MG132-induced apoptosis, which was likely due to impaired autophagic degradation.

MATERIALS AND METHODS

Reagents

MG132, Xestospongin C (Xec), 2-aminoethoxydiphenyl borate (2-APB), and Bafilomycin A1 (BAF) were obtained from Sigma. BAPTA-AM was purchased from Invitrogen. The following antibodies were used for western blot: anti-ATF4/Creb-2 (Santa Cruz, sc-200), anti-Gadd153/CHOP (Santa Cruz, sc-793), anti-Bip/GRP78 (Sigma, G9043), anti-β-Actin (Sigma, A5441), anti-Cleaved Caspase-3 (Cell Signaling, 9661), and anti-GAPDH (Cell Signaling, 2118). The rabbit polyclonal anti-LC3B antibody was made using a peptide representing the NH_2-terminal 14 amino acids of human LC3B and an additional cysteine (PSEKTFKQRRTFEQC) as described previously (13). Anti-Calnexin (Santa Cruz, sc-11397) and anti-Lamp1 antibody, which was from Developmental Studies Hybridoma Bank (University of Iowa), were used for immunostaining. Horseradish peroxidase–conjugated or Cy3-conjugated secondary antibodies were from Jackson ImmunoResearch Lab.

Cell Culture

HCT116 Bax-positive (+), Bax-deficient (−), and stable GFP-LC3 Bax (−) cells were maintained in McCOY's 5A medium (Thermo Scientific), and DU145 prostate cancer cells were maintained in DMEM (Thermo Scientific). All cell lines were maintained with routine supplements (28) in a 37°C incubator with 5% CO_2.

Microscopy Analysis

For fluorescence microscopy studies, cells were cultured on cover slides in 12-well plates and treated as necessary. The cells were fixed with 4% paraformaldehyde (PFA) before microscopy. Fluorescence images were acquired under a fluorescence microscope (Nikon Eclipse TE200) using a Cool SNAPS digital camera (Roper Scientific). Images were acquired and analyzed using MetaMorph software. For immunostaining, fixed cells were immunostained with anti-Lamp1 antibody followed by Cy3-conjugated secondary antibody, or cells were stained with an anti-calnexin and anti-Lamp1 antibody followed by FITC-conjugated and Cy3-conjugated secondary antibodies as previously described (29). The colocalization of GFP-LC3 with Lamp1 or calnexin with Lamp1 was examined using a confocal microscope (Leica TCS SPE). At least 20 cells from each experiment were

analyzed, and at least 3 separate experiments were performed per study. To determine vacuolated cells, HCT116 Bax(−) and Bax (+) and DU145 cells were treated with MG132 (1 μM) in the presence or absence of BAPTA-AM (10 μM or 20 μM) for 12 hours, and images of vacuolated cells were taken using a Nikon Eclipse TE200 microscope and a Cool SNAPS digital camera with MetaMorph software. Vacuoles were counted using cells treated from three separate experiments, and more than 90 cells were counted from each individual experiment. To determine the effect of IP3 receptor inhibition on cellular vacuolization, HCT116 Bax (−) cells were treated with MG132 (1 μM) in the presence or absence of Xec (25 nM)f or 2-APB (20 μM) for 12 hours, and images of vacuolated cells were taken using a Nikon Eclipse TE200 microscope and a Cool SNAPS digital camera with MetaMorph software. Vacuoles were counted using cells treated from two separate experiments, and more than 200 cells were counted from each individual experiment. To determine apoptotic cell death, HCT116 Bax (+) cells were treated with MG132 (1 μM), BAPTA-AM (10 μM), or BAF (50 nM) for 20 hours. Cells were stained with Hoechst 33342 (1 μg/mL, Invitrogen), and digital images were obtained using a fluorescence microscope (Nikon Eclipse TE200). Fragmented and condensed apoptotic nuclei were quantified, and results were expressed as percent of apoptotic cells. For Electron Microscopy, cells were fixed with 2% glutaraldehyde in 0.1M phosphate buffer (pH 7.4) followed by 1% OsO_4. After dehydration, thin sections were stained with uranyl acetate and lead citrate for observation under a JEM 1016CX electron microscope.

Analysis of Intracellular Calcium Levels

500,000 HCT116 Bax (−) and DU145 cells were plated in a 6-well plate and left overnight. Cells were then treated with MG132 (1 μM) in the presence or absence of BAPTA-AM (10 μM), Xec (25 nM), or 2-APB (20 μM) for 16 hours. Cells were tryspinized and washed with calcium-free Hank's buffer (HBSS) before staining with 2.5 μM Fluo-4 AM (Invitrogen) in HBSS for 30 minutes. Cells were washed and resuspended in HBSS before measurement of Fluo-4 green fluorescence intensity by flow cytometry.

Analysis of Proteasome Activity

HCT116 Bax (−) cells were treated with MG132 (0.25, 0.5, or 1 μM), BAPTA-AM (10 μM), or BAF (50 nM) for 16 hours before isolation of total protein lysate using RIPA buffer. Total cell lysate (10 μg) was used for proteasome activity analysis using Suc-LLVY-AMC substrate (Enzo). Briefly, lysates were diluted to 10 μg each in 15 μL of RIPA buffer and added to a white 96-well flat bottom plate. AMC substrate (20 nM) was added to each well along with 100 μL of assay buffer (50 mM Tris pH 7.5, 25 mM KCL, 10 mM NaCI, and 1 mM $MgCI_2$ diluted in dH_2O). Proteasome activity was determined by measuring AMC release using an excitation/emission 380/460 test filter on a Tecan plate reader after 1 hour. Data were expressed as percent of proteasome activity compared to untreated-control. At least three separate experiments were performed for analysis of proteasome activity.

Western Blot

HCT116 Bax (−) or Bax (+) cells were treated with MG132 (1μM), BAPTA-AM (10μM), or BAF (50 nM) for 20 hours before isolation of total protein lysate using RIPA buffer. Protein (20 μg) was separated by a 12% SDS-PAGE gel before transfer to a PVDF membrane. Membranes were probed using indicated primary and secondary antibodies and developed with SuperSignal West Pico chemiluminescent substrate (Pierce).

Statistical Analysis

Experimental data were subjected to a student's Two-tailed T-test or to a Rank Sum test to analyze differences between two groups. A one-way ANOVA was used to analyze differences among multiple groups.

RESULTS

MG132-induced Proteasome Inhibition Increased Intracellular Calcium Levels

We have previously shown that proteasome inhibition by MG132 induces ER stress that can result in Bax-dependent apoptotic and Bax-independent non-apoptotic cell death (5). Therefore, HCT116 Bax (−) and Bax (+) cells were both used to investigate the effect of MG132-induced proteasome inhibition on intracellular calcium levels.

To determine the effect of proteasome inhibition by MG132 on intracellular calcium, HCT116 Bax (−) cells were treated with MG132 (1 μM) in the presence or absence of the calcium chelator BAPTA-AM (10 μM) for 16 hours. Proteasome inhibition by MG132 resulted in increased levels of intracellular calcium as demonstrated by Fluo-4-AM fluorescence intensity analysis (Figure 1A), and MG132 induced a 2-fold increase in Fluo-4-AM fluorescence intensity compared to untreated-control (Supplemental Figure 1A). This increase in intracellular calcium induced by MG132 was returned to untreated-control levels when MG132 treatment was combined with BAPTA-AM (Figure 1A). We also treated DU145 cells with MG132 (1 μM) in the presence or absence of BAPTA-AM (10 μM) for 16 hours, which produced similar results to HCT116 cells (Supplemental Figure 1B).

To ensure that MG132 was inhibiting proteasome activity, HCT116 Bax (+) and Bax (−) cells were treated with varying concentrations of MG132 (0.25, 0.5, and 1 μM), and total protein lysates were analyzed for proteasome activity. Proteasome activity was significantly decreased in MG132 treated cells compared to untreated-control cells, as expected (Figure 1B). In addition, MG132 decreased proteasome activity regardless of the presence or absence of Bax. Inhibition of proteasome activity was similar among all concentrations of MG132 with an average of 42% proteasome activity for Bax (−) cells and 35% proteasome activity for Bax (+) cells compared to untreated-control cells (Figure 1B). Therefore, 1 μM or 0.5 μM of MG132 was used for additional experiments.

To determine if chelating calcium with BAPTA-AM had any effect on proteasome activity, we treated HCT116 Bax (−) cells with MG132 (1 μM) in the presence or absence of BAPTA-AM (10 μM) for 16 hours, and total protein lysates were analyzed for proteasome activity (Figure 1C). Treatment with MG132 decreased proteasome activity 52% compared to untreated-control, as expected (Figure 1C). However, calcium chelation by BAPTA-AM (10 μM) alone did not affect proteasome activity compared to untreated-control cells or when combined with MG132 compared to MG132 alone (Figure 1C).

BAF, a potent and specific inhibitor of vacuolar H+ ATPase (V-ATPase), inhibits autolysosome and lysosome function (30). To determine whether inhibition of lysosome function affects MG132-induced proteasome inhibition, HCT116 Bax (−) cells were treated with BAF (50 nM) for 16 hours in the presence or absence of MG132 (1 μM). BAF-induced autophagy inhibition did not affect proteasome activity compared to untreated-control cells or when combined with MG132 compared to MG132 alone (Figure 1C).

Chelation of MG132-induced Intracellular Calcium Surge Protected against ER Stress

Proteasome inhibition is known to cause cellular vacuolization due to ER stress (5, 9). To determine whether increased intracellular calcium is important for MG132-induced cellular

vacuolization and ER stress, HCT116 cells were treated with 1 μM MG132 in the presence or absence of 10 μM BAPTA-AM for 16 hours. As shown in Figure 2, chelating calcium with BAPTA-AM significantly decreased MG132-induced cellular vacuole formation regardless of the presence of Bax (Figures 2A and 2B). In addition, BAPTA-AM also inhibited MG132-induced cellular vacuolization in DU145 prostate cancer cells (Supplemental Figure 2A and 2B). These data indicate that the increased intracellular calcium levels induced by MG132 were responsible for cellular vacuolization.

ER is the major calcium store in the cell, and the IP3 receptor allows for release of calcium from the ER, which can be suppressed by Xestospongin C (Xec) or 2-aminoethoxydiphenyl borate (2-APB) (31, 32). To determine whether IP3 receptor mediated ER calcium release would be responsible for MG132-induced increased intracellular calcium, HCT116 Bax (−) cells were treated with MG132 (1 μM) in combination with 25 nM of Xec or 20 μM of 2-APB. Neither Xec nor 2-APB reduced cellular vacuolization induced by MG132 (Supplemental Figure 3A and 3B). In addition, intracellular calcium levels were similar between cells treated with MG132 in combination with Xec or 2-APB to cells treated with MG132 alone, as indicated by Fluo-4-AM fluorescence intensity analysis (Supplemental Figures 3C and 3D). These data suggest that the ER was less likely the source of increased intracellular calcium induced by MG132. To determine if MG132 increased intracellular calcium by increasing extracellular calcium influx, EGTA was used to chelate extracellular calcium. EGTA did not affect cellular vacuolization induced by MG132 (Supplemental Figure 3E), indicating that influx of extracellular calcium was most likely not the source for the increase in intracellular calcium induced by MG132. These data suggest that the increase in intracellular calcium was not due to calcium release from the ER or due to an increase in extracellular calcium influx.

In addition to promoting cellular vacuolization, proteasome inhibitor-induced ER stress also triggers the UPR. To further determine whether increased intracellular calcium also affects the UPR, HCT116 Bax (−) cells were treated with MG132 (1 μM) in the presence or absence of BAPTA-AM (10 μM) for 16 hours, and total protein lysates were analyzed by western blot for expression of UPR proteins including Bip, CHOP, and ATF4 (5, 9). MG132-induced proteasome inhibition caused increased protein expression of Bip, CHOP, and ATF4, indicating increased ER stress. Calcium chelation with BAPTA-AM decreased expression levels for all of these UPR proteins to levels similar to untreated-control cells when added in combination with MG132 compared to MG132 treatment alone (Figure 2C). These results indicate that increased intracellular calcium levels caused by proteasome inhibition can induce ER stress and the UPR response.

To confirm that the cellular vacuolization seen in Figure 2 was caused by ER dilation, HCT116 Bax (−) cells were treated with MG132 and immunostained for the ER chaperone protein, Calnexin, and for the lysosome protein, Lamp1 As shown in Figure 3A, vacuoles induced by MG132 treatment stained positive for calnexin, but this calnexin staining did not co-localize with Lamp1 staining, indicating that vacuoles formed from the ER, but not from lysosomes. ER dilation was also seen in DU145 cells treated with MG132 (Supplemental Figure 4). This vacuolization from the ER was confirmed by electron microscopy in HCT116 Bax (−) cells (Figure 3B). Untreated-control cells did not have vacuolization (Figure 3B, **panel a**). However, treatment with MG132 induced dilation of the nuclear membrane and vacuole formation (Figure 3B, **panels b and c**). The nuclear membrane is known to be part of the ER membrane (**panel c, arrow**); therefore, these results support that vacuoles were derived from the ER. ER dilation was decreased by BAPTA-AM treatment (Figure 3B, panel d), indicating that increased intracellular calcium levels caused by proteasome inhibition led to ER dilation and ER stress, and chelation of this intracellular

calcium with BAPTA-AM protected against induction of ER stress induced by proteasome inhibition.

Calcium Chelation during ER Stress Increased Apoptosis

We next determined whether chelation of intracellular calcium by BAPTA-AM inhibited MG132-induced apoptosis. HCT116 Bax (+) cells were treated with 1 μM MG132 with or without 10 μM of BAPTA-AM for 20 hours, and cells were analyzed for apoptosis by Hoechst staining and by western blot analysis for cleaved activated caspase-3. MG132 treatment caused approximately 20% apoptosis, which was increased 4-fold over untreated-control treatment (5% apoptosis). BAPTA-AM alone also caused approximately 12% apoptosis, a 2.4-fold increase compared to untreated-control. Furthermore, BAPTA-AM treatment caused an approximate 30% increase in apoptosis when combined with MG132 treatment, which was an additional increase in apoptosis greater than that induced by MG132 or BAPTA-AM treatment alone (Figure 4A, 4B). Therefore, BAPTA-AM in combination with MG132 enhanced cell death even though BAPTA-AM significantly inhibited MG132-induced ER stress under the same conditions (Figures 2 and 3). We previously showed that inhibition of autophagy by using genetic knockdown of autophagy genes or pharmacological inhibitors, such as 3-methyladenine, further enhanced proteasome inhibition-induced cell death (9).In line with these previous findings, BAF treatment in combination with MG132 caused approximately 27% cell death, which was a slight increase in cell death compared to MG132 treatment alone (Figure 4A, 4B). Consistent with results for apoptotic nuclei, MG132 induced cleavage of caspase-3 (Figure 4C). BAPTA-AM did not induce caspase-3 cleavage alone, but it caused greater cleavage of caspase-3 when combined with MG132 compared to MG132 treatment alone (Figure 4C). In addition, MG132 treatment in combination with BAF also increased the cleavage of caspase-3 (Figure 4C) compared to MG132 treatment alone. Therefore, even though chelating calcium with BAPTA-AM treatment reduced ER stress, it exacerbated cell death via apoptosis. Inhibition of lysosomal functions by BAF also enhanced MG132-induced apoptosis in HCT116 cells.

Chelation of Calcium via BAPTA-AM did not affect the Colocalization of GFP-LC3 Puncta with the Lysosomal Marker Lamp1

Because intracellular calcium has been implicated in the fusion of autophagosomes with lysosomes, we next asked whether the failure of BAPTA-AM to inhibit MG132-induced apoptosis was due to impaired fusion of autophagosomes with lysosomes, which would in turn impair autophagic degradation. HCT116 GFP-LC3 expressing cells were treated with MG132 (0.5 μM) in the presence or absence of BAPTA-AM (10 M) for 16 hours and immunostained with LAMP1 to determine colocalization of autophagosomes (GFP-LC3 positive vesicles) with lysosomes (Lamp1 positive vesicles). All experimental groups had an average of approximately 50% colocalization of GFP-LC3 puncta with Lamp1, which is represented as yellow fluorescent dots (Figure 5A, 5B), indicating that calcium chelation by BAPTA-AM had no effect on colocalization of autophagosomes with lysosomes in HCT116 cells.

Chelation of Calcium via BAPTA-AM Impaired MG132-Induced Autophagy

Proteasome inhibition induces autophagy, and inhibition of autophagy can sensitize proteasome inhibitor-induced cell death (9, 13). We observed that BAPTA-AM also enhanced MG132-induced apoptosis similar to BAF, so we next determined the effect of BAPTA-AM on MG132-induced autophagy. Autophagy is a dynamic process, and it is well known that both GFP-LC3 and LC3-II proteins are degraded after fusion of autophagosomes with lysosomes. Therefore, inhibition of autophagic degradation can often lead to the accumulation of LC3-II proteins and GFP-LC3 puncta (33, 34). Similar to BAF, BAPTA-AM alone slightly increased the number of GFP-LC3 puncta compared to untreated-control

cells. More importantly, co-treatment of BAPTA-AM with MG132 or co-treatment of BAF with MG132 further enhanced the number of GFP-LC3 puncta compared to either treatment alone (Figure 6A–C). Consistent with the GFP-LC3 puncta data, EM studies confirmed the accumulation of autophagosome/autolysosome structures in cells treated with MG132 or BAPTA-AM alone as well as in MG132 and BAPTA-AM co-treated cells (Figure 6D). Moreover, western blot analysis revealed that BAPTA-AM also further increased MG132-induced LC3-II levels (Figure 6E), indicating that BAPTA-AM may suppress LC3-II turnover, which likely reflects impaired autophagic degradation. Interestingly, treatment with BAPTA-AM in combination with BAF produced similar levels of LC3-II protein as treatment with BAF alone, and combined treatment with BAPTA-AM, BAF, and MG132 did not further increase LC3-II protein levels above treatment with MG132 + BAF alone (Figure 6F). Therefore, these data suggest that BAPTA-AM likely inhibits lysosome function in a similar fashion to BAF.

DISCUSSION

Autophagy is a specific catabolic pathway that plays an important role in regulating the homeostasis of cellular proteins and organelles. Tumor cells often use autophagy as a cell survival mechanism. Therefore, targeting autophagy has become a novel and effective therapeutic target (15, 35). Inhibition of the UPS, another cellular protein degradation pathway, has been demonstrated as an effective therapeutic target for treating cancers. However, resistance to proteasome inhibitors has developed in some patients. We and others have previously demonstrated that inhibition of the UPS by various proteasome inhibitors also induces autophagy as a compensatory cell survival mechanism by relieving proteasome inhibitor-induced ER stress (9, 10). Combined targeting of the UPS and autophagy has become a potent strategy in cancer treatment, and several clinical trials using this approach are ongoing (15).

In the present study, we found that inhibition of the UPS by MG132 induced ER stress, which was mainly mediated by a rise in intracellular calcium levels. BAPTA-AM, a cell permeable intracellular calcium chelator, inhibited this MG132-induced increase in intracellular calcium and subsequently suppressed MG132-induced ER stress. To our surprise, BAPTA-AM did not protect against MG132-induced apoptosis. The lack of protection against MG132-induced apoptosis was possibly due to impaired autophagy/lysosome function caused by treatment with MG132 and BAPTA-AM. Thus, our results reveal a novel mechanism suggesting that calcium homeostasis could be an important factor for normal autophagy/lysosome function.

The ER is the most important intracellular calcium store. The concentration of calcium in the ER can reach up to 0.5–2 mM, while its cytoplasmic concentration is as low as 100–300 nM in resting cells (36, 37). The high luminal calcium concentration in the ER is a critical factor for determining the activity of synthesis and processing of proteins within the ER (12). Therefore, disturbance of intracellular calcium homeostasis triggers the ER stress response. Moreover, ER stress often leads to activation of the UPR as a major protective and compensatory mechanism to relieve ER stress. One of the major functions of the UPR is to selectively up-regulate some ER chaperone proteins by activating a number of bZip transcription factors to assist with proper protein folding while simultaneously shutting down general protein synthesis. If the stress is too severe for ER function to fully recover by compensatory mechanisms, ER stress can also trigger cell death. In addition to ER-associated proteasome degradation and the UPR, we and others have recently demonstrated that induction of autophagy can also serve as another compensatory mechanism to relieve ER stress. Notably, inhibition of autophagy further exacerbates ER stress and ER stress-associated cell death (9, 38).

In the present study, we found that inhibition of the proteasome by MG132 increased intracellular calcium levels. Our data suggest that neither ER nor extracellular calcium influx were sources for this MG132-induced intracellular calcium increase. We speculate that the source of calcium increased by MG132 could be mitochondria because mitochondria are another important site for calcium storage in the cell (39). However, due to a lack of reliable quantitative methods for measurement and blocking of mitochondrial Ca2+ release, future studies are needed to test this hypothesis. Nevertheless, the finding that BAPTA-AM inhibited the MG132-induced rise of intracellular calcium, intracellular vacuolization, and the UPR response suggests that an intracellular calcium surge plays an important role in MG132-induced ER stress. Intriguingly, although BAPTA-AM efficiently inhibited MG132-induced ER stress, BAPTA-AM did not attenuate, but rather exacerbated, MG132-induced apoptosis. These results suggest that BAPTA-AM might also inhibit other cellular protective mechanisms induced by MG132, such as autophagy, in addition to inhibiting the UPR response. We found that BAPTA- AM impaired the autophagy process similar to BAF, a lysosomal inhibitor. This notion is supported by the observations that both BAPTA-AM and BAF further increased the number of GFP-LC3 puncta and LC3-II protein levels when combined with MG132 compared to MG132 alone.

Autophagy is a dynamic process that requires the stepwise maturation of autophagosomes through the fusion of autophagosomes with lysosomes, which allows autophagic degradation of enwrapped cargo using lysosomal proteases. Emerging evidence has implicated that calcium may play an important role in regulating autophagosome-lysosome fusion, although its exact role is controversial. Using isolated endosomes and lysosomes from rat hepatocytes in a cell free system, it was demonstrated that calcium located within organelles is required for the fusion of endosomes with lysosomes, because this fusion was suppressed by the membrane permeable calcium chelator BAPTA-AM (25). When intracellular calcium levels were modulated by distinct mechanisms including BAPTA-AM, calcium ionophores, and calcium releasing agents in primary rat hepatocytes, autophagy was suppressed, suggesting that the autophagic process is dependent on the presence of intracellular sequestered calcium (40). Moreover, a recent study showed that elevated intracellular calcium levels caused by thapsigargin-induced release of ER calcium stores blocked autophagosome-lysosome fusion due to alterations of cellular localization of Rab7 (26). However, we found that the colocalization of GFP-LC3 (autophagosome marker) with Lamp1 (a lysosomal marker) was similar with MG132 treatment alone or in combination with BAPTA-AM, suggesting that neither MG132 nor BAPTA-AM affect the fusion of autophagosomes with lysosomes. We also found that MG132 alone or in combination with BAPTA-AM did not affect Rab7 colocalization with GFP-LC3 positive vesicles (data not shown). It is currently unclear why MG132 did not affect the fusion of autophagosomes with lysosomes when it has previously been shown to be impaired by thapsigargin. While different cell types could be one reason for this discrepancy, it is possible that different sources for the surge of intracellular calcium induced by different stimuli could produce different outcomes. Nevertheless, we found that the number of GFP-LC3 puncta and LC3-II levels, as well as accumulation of autophagosomes in HCT116 cells, were increased by BAPTA-AM and further enhanced when BAPTA-AM was combined with MG132. These findings are quite similar to the lysosomal inhibitor BAF, suggesting that BAPTA-AM may directly impair lysosomal function. It is known that BAF inhibits lysosome function by inhibiting the vacuolar ATPase. While it is not currently clear whether BAPTA-AM would also impair the vacuolar ATPase, disruption of lysosome calcium homeostasis by BAPTA-AM might also contribute to its inhibition of lysosome function. Niemann-Pick type C (NPC) disease is a lysosomal storage disease characterized by selective loss of cerebellar Purkinje neurons. This disease is caused by mutation of genes important for regulating lysosomal calcium homeostasis (41). It remains to be determined if BAPTA-AM also decreases lysosomal calcium levels and

impairs lysosomal function, which could account for the enhanced cell death in MG132-treated cells.

In conclusion, we found that MG132 inhibited proteasome activity in human colon cancer HCT116 cells, which led to a rise in intracellular calcium levels and ER stress. BAPTA-AM inhibited the MG132-induced rise of intracellular calcium and ER stress, but failed to rescue MG132-induced apoptosis, which was likely due to impaired autophagy-lysosomal degradation.

Supplementary Material

Refer to Web version on PubMed Central for supplementary material.

Acknowledgments

The research work in W.X Ding's lab was supported in part by the NIAAA funds R01 AA020518-01 and National Center for Research Resources (5P20RR021940-07). J. A. Williams was supported by the "Training Program in Environmental Toxicology" [grant 5 T32 ES007079] from the National Institute of Environmental Health Sciences. Y.F. Hou was supported by the National Natural Science Foundation of China (# 81072165) and the Shanghai Science and Technology Committee (# 09PJ1402700). The authors are indebted to Dr. Bert Vogelstein (Johns Hopkins University) and Lin Zhang (University of Pittsburgh) for the HCT116 Bax-positive and Bax-negative cell lines.

Abbreviations

2-APB	2-aminoethoxydiphenyl borate
BAF	Bafilomycin A1
BAPTA-AM	1,2-bis-(o-aminophenoxy)-ethane-N,N,N',N'-tetraacetic acid, tetraacetoxymethyl esteris
CPP	calcium phosphate precipitates
eIF2-alpha	Eukaryotic Translation Initiation Factor 2-alpha
ER	Endoplasmic Reticulum
IRE1	Inositol-requiring Enzymel
JNK	c-Jun N-terminal Kinase
LC3	microtubule-associated protein 1 light chain 3
MEF	mouse embryonic fibroblasts
PFA	paraformaldehyde
PE	Phosphatidylethanolamine
PERK	Protein Kinase RNA-like Endoplasmic Reticulum Kinase
UPR	Unfolded Protein Response
UPS	Ubiquitin Proteasome System
Xec	Xestospongin C

References

1. Hershko A, Ciechanover A. The ubiquitin system. Annu Rev Biochem. 1998; 67:425–479. [PubMed: 9759494]

2. Mitchell BS. The proteasome-an emerging therapeutic target in cancer. N Engl J Med. 2003 Jun 26; 348(26):2597–2598. [PubMed: 12826633]
3. Adams J. The development of proteasome inhibitors as anticancer drugs. Cancer Cell. 2004 May; 5(5):417–421. [PubMed: 15144949]
4. Chauhan D, Hideshima T, Anderson KC. Proteasome inhibition in multiple myeloma: therapeutic implication. Annu Rev Pharmacol Toxicol. 2005; 45:465–476. [PubMed: 15822185]
5. Ding WX, Ni HM, Yin XM. Absence of Bax switched MG132-induced apoptosis to non-apoptotic cell death that could be suppressed by transcriptional or translational inhibition. Apoptosis : an international journal on programmed cell death. 2007 Dec; 12(12):2233–4444. [PubMed: 17912641]
6. Levine B, Klionsky DJ. Development by self-digestion: molecular mechanisms and biological functions of autophagy. Dev Cell. 2004 Apr; 6(4):463–477. [PubMed: 15068787]
7. Lum JJ, DeBerardinis RJ, Thompson CB. Autophagy in metazoans: cell survival in the land of plenty. Nat Rev Mol Cell Biol. 2005 Jun; 6(6):439–448. [PubMed: 15928708]
8. Kamada Y, Sekito T, Ohsumi Y. Autophagy in yeast: a TOR-mediated response to nutrient starvation. CurrTop Microbiol Immunol. 2004; 279:73–84.
9. Ding WX, Ni HM, Gao W, Yoshimori T, Stolz DB, Ron D, et al. Linking of autophagy to ubiquitin-proteasome system is important for the regulation of endoplasmic reticulum stress and cell viability. Am J Pathol. 2007 Aug; 171(2):513–524. [PubMed: 17620365]
10. Zhu K, Dunner K Jr, McConkey DJ. Proteasome inhibitors activate autophagy as a cytoprotective response in human prostate cancer cells. Oncogene. 2010 Jan 21; 29(3):451–462. [PubMed: 19881538]
11. Komatsu M, Waguri S, Chiba T, Murata S, Iwata J, Tanida I, et al. Loss of autophagy in the central nervous system causes neurodegeneration in mice. Nature. 2006 Jun 15; 441(7095):880–884. [PubMed: 16625205]
12. Michalak M, Robert Parker JM, Opas M. Ca2+ signaling and calcium binding chaperones of the endoplasmic reticulum. Cell Calcium. 2002 Nov-Dec;32(5–6):269–278. [PubMed: 12543089]
13. Ding WX, Ni HM, Gao W, Chen X, Kang JH, Stolz DB, et al. Oncogenic transformation confers a selective susceptibility to the combined suppression of the proteasome and autophagy. Mol Cancer Ther. 2009 Jul; 8(7):2036–2045. [PubMed: 19584239]
14. Avivar-Valderas A, Salas E, Bobrovnikova-Marjon E, Diehl JA, Nagi C, Debnath J, et al. PERK integrates autophagy and oxidative stress responses to promote survival during extracellular matrix detachment. Mol Cell Biol. 2011 Sep; 31(17):3616–3629. [PubMed: 21709020]
15. Amaravadi RK, Lippincott-Schwartz J, Yin XM, Weiss WA, Takebe N, Timmer W, et al. Principles and current strategies for targeting autophagy for cancer treatment. Clin Cancer Res. 2011 Feb 15; 17(4):654–666. [PubMed: 21325294]
16. Thastrup O, Cullen PJ, Drobak BK, Hanley MR, Dawson AP. Thapsigargin, a tumor promoter, discharges intracellular Ca2+ stores by specific inhibition of the endoplasmic reticulum Ca2(+)-ATPase. Proc Natl Acad Sci USA. 1990 Apr; 87(7):2466–2470. [PubMed: 2138778]
17. Hoyer-Hansen M, Bastholm L, Szyniarowski P, Campanella M, Szabadkai G, Farkas T, et al. Control of macroautophagy by calcium, calmodulin-dependent kinase kinase-beta, and Bcl-2. Mol Cell. 2007 Jan 26; 25(2):193–205. [PubMed: 17244528]
18. Gao W, Ding WX, Stolz DB, Yin XM. Induction of macroautophagy by exogenously introduced calcium. Autophagy. 2008 Aug; 4(6):754–761. [PubMed: 18560273]
19. Sarkar S, Korolchuk V, Renna M, Winslow A, Rubinsztein DC. Methodological considerations for assessing autophagy modulators: a study with calcium phosphate precipitates. Autophagy. 2009 Apr; 5(3):307–313. [PubMed: 19182529]
20. Williams A, Sarkar S, Cuddon P, Ttofi EK, Saiki S, Siddiqi FH, et al. Novel targets for Huntington's disease in an mTOR-independent autophagy pathway. Nat Chem Biol. 2008 May; 4(5):295–305. [PubMed: 18391949]
21. Itakura E, Kishi-Itakura C, Mizushima N. The hairpin-type tail-anchored SNARE syntaxin 17 targets to autophagosomes for fusion with endosomes/lysosomes. Cell. 2012 Dec 7; 151(6):1256–1269. [PubMed: 23217709]

22. Jager S, Bucci C, Tanida I, Ueno T, Kominami E, Saftig P, et al. Role for Rab7 in maturation of late autophagic vacuoles. J Cell Sci. 2004 Sep 15; 117(Pt 20):4837–4848. [PubMed: 15340014]
23. Rusten TE, Stenmark H. How do ESCRT proteins control autophagy? J Cell Sci. 2009 Jul l; 122(Pt 13):2179–2183. [PubMed: 19535733]
24. Eskelinen EL, lllert AL, Tanaka Y, Schwarzmann G, Blanz J, Von Figura K, et al. Role of LAMP-2 in lysosome biogenesis and autophagy. Mol Biol Cell. 2002 Sep; 13(9):3355–3368. [PubMed: 12221139]
25. Pryor PR, Mullock BM, Bright NA, Gray SR, Luzio JP. The role of intraorganellar Ca(2+) in late endosome-lysosome heterotypic fusion and in the reformation of lysosomes from hybrid organelles. J Cell Biol. 2000 May 29; 149(5):1053–1062. [PubMed: 10831609]
26. Ganley IG, Wong PM, Gammoh N, Jiang X. Distinct autophagosomal-lysosomal fusion mechanism revealed by thapsigargin-induced autophagy arrest. Mol Cell. 2011 Jun 24; 42(6):731–743. [PubMed: 21700220]
27. Li X, Yang D, Li L, Peng C, Chen S, Le W. Proteasome inhibitor lactacystin disturbs the intracellular calcium homeostasis of dopamine neurons in ventral mesencephalic cultures. Neurochemistry international. 2007 Jun; 50(7–8):959–965. [PubMed: 17561309]
28. Zhang L, Yu J, Park BH, Kinzler KW, Vogelstein B. Role of BAX in the apoptotic response to anticancer agents. Science. 2000 Nov 3; 290(5493):989–992. [PubMed: 11062132]
29. Ding WX, Guo F, Ni HM, Bockus A, Manley S, Stolz DB, et al. Parkin and mitofusins reciprocally regulate mitophagy and mitochondrial spheroid formation. J Biol Chem. 2012 Dec 7; 287(50): 42379–42388. [PubMed: 23095748]
30. Yamamoto A, Tagawa Y, Yoshimori T, Moriyama Y, Masaki R, Tashiro Y. Bafilomycin Al prevents maturation of autophagic vacuoles by inhibiting fusion between autophagosomes and lysosomes in rat hepatoma cell line, H-4-II-E cells. Cell Struct Funct. 1998 Feb; 23(l):33–42. [PubMed: 9639028]
31. Mikoshiba K. IP3 receptor/Ca2+ channel: from discovery to new signaling concepts. Journal of neurochemistry. 2007 Sep; 102(5):1426–1446. [PubMed: 17697045]
32. Peppiatt CM, Collins TJ, Mackenzie L, Conway SJ, Holmes AB, Bootman MD, et al. 2-Aminoethoxydiphenyl borate (2-APB) antagonises inositol 1,4,5-trisphosphate-induced calcium release, inhibits calcium pumps and has a use-dependent and slowly reversible action on store-operated calcium entry channels. Cell Calcium. 2003 Jul; 34(l):97–108. [PubMed: 12767897]
33. Ni HM, Bockus A, Wozniak AL, Jones K, Weinman S, Yin XM, et al. Dissecting the dynamic turnover of GFP-LC3 in the autolysosome. Autophagy. 2011 Feb; 7(2):188–204. [PubMed: 21107021]
34. Klionsky DJ, Abdalla FC, Abeliovich H, Abraham RT, Acevedo-Arozena A, Adeli K, et al. Guidelines for the use and interpretation of assays for monitoring autophagy. Autophagy. 2012 Apr; 8(4):445–544. [PubMed: 22966490]
35. Ni HM, Williams JA, Yang H, Shi YH, Fan J, Ding WX. Targeting autophagy for the treatment of liver diseases. Pharmacol Res. 2012 Dec; 66(6):463–474. [PubMed: 22871337]
36. Rossi D, Barone V, Giacomello E, Cusimano V, Sorrentino V. The sarcoplasmic reticulum: an organized patchwork of specialized domains. Traffic. 2008 Jul; 9(7):1044–1049. [PubMed: 18266914]
37. Burdakov D, Petersen OH, Verkhratsky A. Intraluminal calcium as a primary regulator of endoplasmic reticulum function. Cell Calcium. 2005 Sep-Oct;38(3–4):303–310. [PubMed: 16076486]
38. Ding WX, Ni HM, Gao W, Hou YF, Melan MA, Chen X, et al. Differential effects of endoplasmic reticulum stress-induced autophagy on cell survival. J Biol Chem. 2007 Feb 16; 282(7):4702–4710. [PubMed: 17135238]
39. Starkov AA. The molecular identity of the mitochondrial Ca2+ sequestration system. The FEBS journal. 2010 Sep; 277(18):3652–3663. [PubMed: 20659159]
40. Gordon PB, Holen I, Fosse M, Rotnes JS, Seglen PO. Dependence of hepatocytic autophagy on intracellularlysequestered calcium. J Biol Chem. 1993 Dec 15; 268(35):26107–26112. [PubMed: 8253727]

41. Lloyd-Evans E, Platt FM. Lysosomal Ca(2+) homeostasis: role in pathogenesis of lysosomal storage diseases. Cell Calcium. 2011 Aug; 50(2):200–205. [PubMed: 21724254]

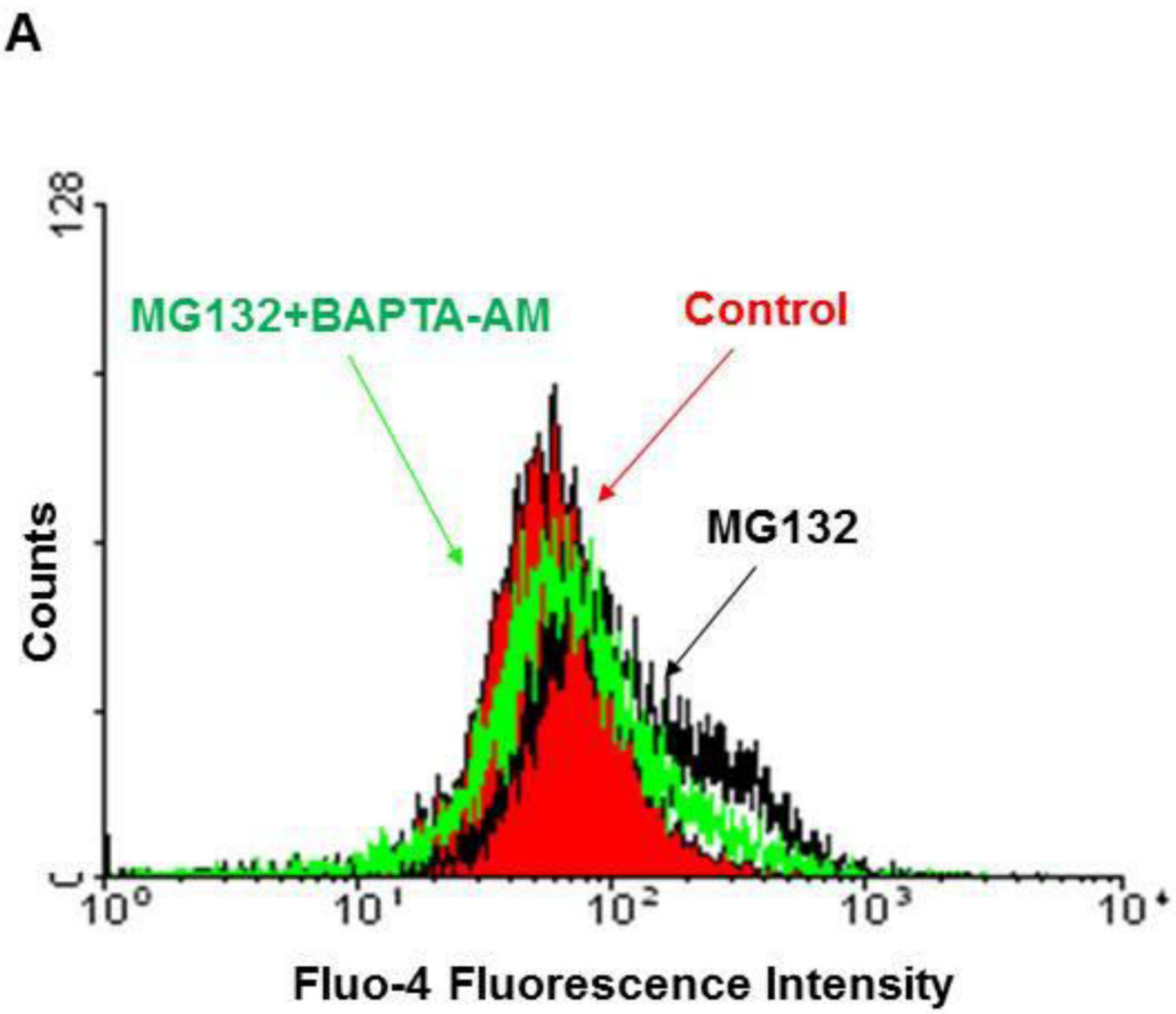

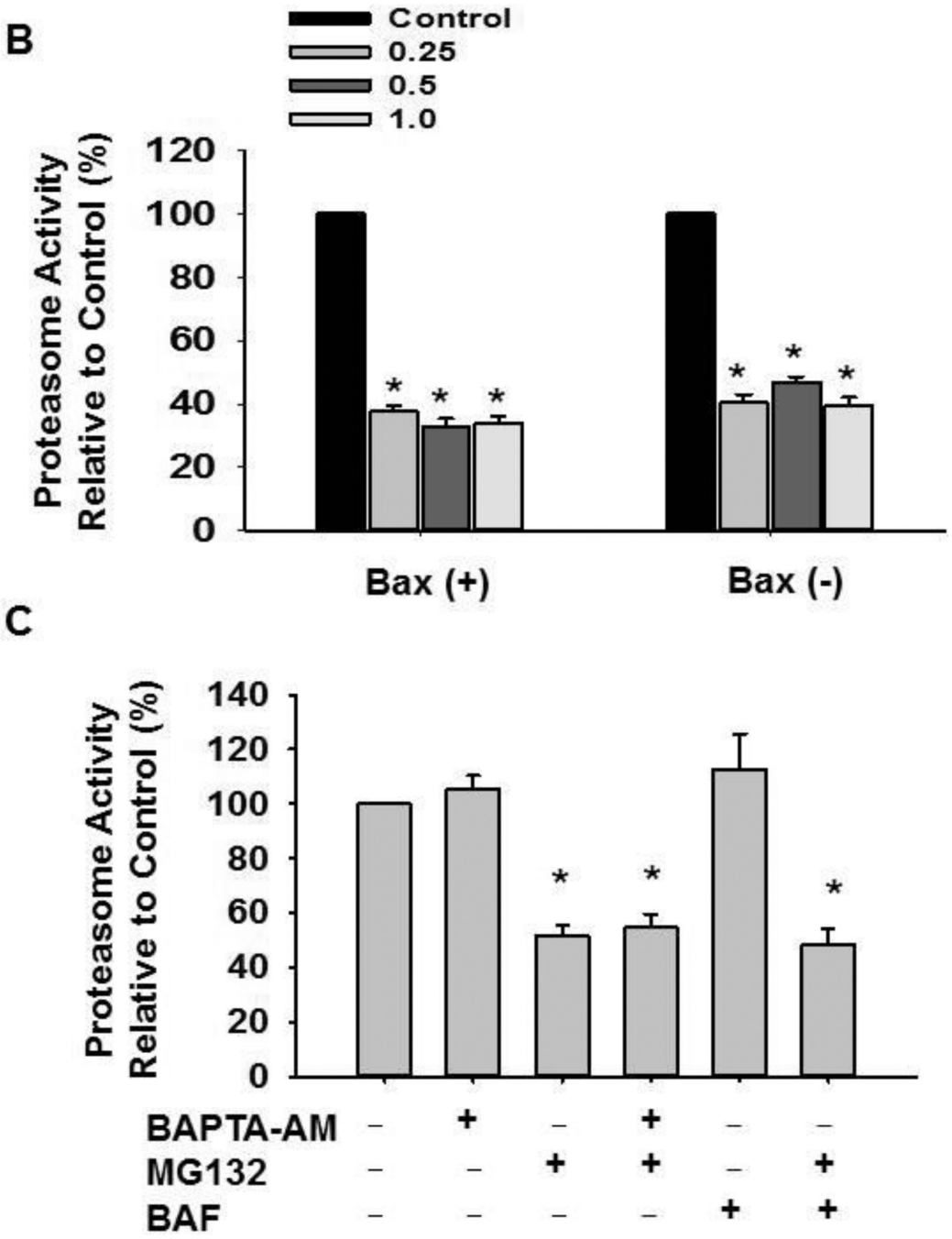

Figure 1. Inhibition of the proteasome by MG132 increased intracellular calcium levels, which was inhibited by BAPTA-AM treatment

HCT116 Bax (−) cells were treated with MG132 (1μM) in the absence or presence of BAPTA-AM (10 μM) for 16 hours. Cells were then stained with 2.5 μM of Fluo-4-AM in calcium-free Hank's buffer for 30 minutes followed by flow cytometry analysis. Representative histogram data are shown in (**A**). (**B**) HCT116 Bax (−) and Bax (+) cells were treated with varying concentrations of MG132 (0.25, 0.5, and 1 μM) for 16 hours, and total protein lysate was used for analysis of proteasome activity using AMC substrate. Results are presented as percent proteasome activity compared to untreated-control (*p<0.01, 2-tailed T-test). (C) HCT116 Bax (−) cells were treated with BAPTA-AM (10

μM), MG132 (1 μM), and BAF (50 nM) for 20 hours, and total protein lysate was used for proteasome activity analysis. Results are expressed as percent proteasome activity compared to untreated-control (*$p<0.05$, One Way ANOVA).

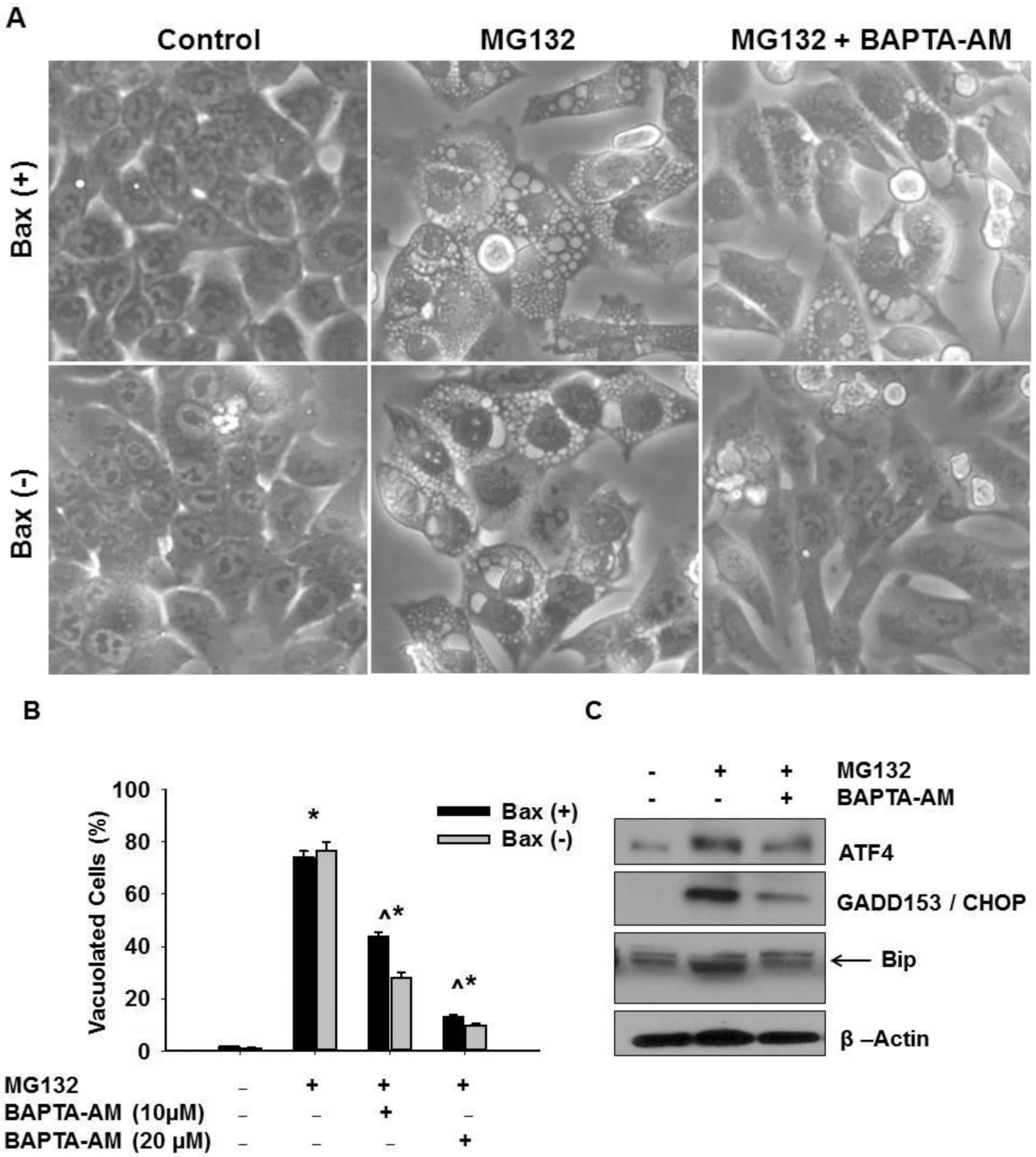

Figure 2. BAPTA-AM inhibited MG132-induced cellular vacuolization

HCT116 Bax (−) and Bax (+) cells were treated with MG132 (1 μM) in the presence or absence of BAPTA-AM (10 μM) for 12 hours followed by phase-contrast microscopy. Representative images are presented in (**A**). (**B**) Vacuolated cells were counted, and results

are expressed as percent of vacuolated cells (*p<0.05 vs untreated-control; ^ p<0.05 vs MG132, One Way ANOVA). (**C**) HCT116 Bax (−) cells were treated with MG132 (1μM) in the presence or absence of BAPTA-AM (10 μM) for 16 hours, and total protein lysates were subjected to western blot analysis. Bip is the lower band on the western blot (arrow).

A

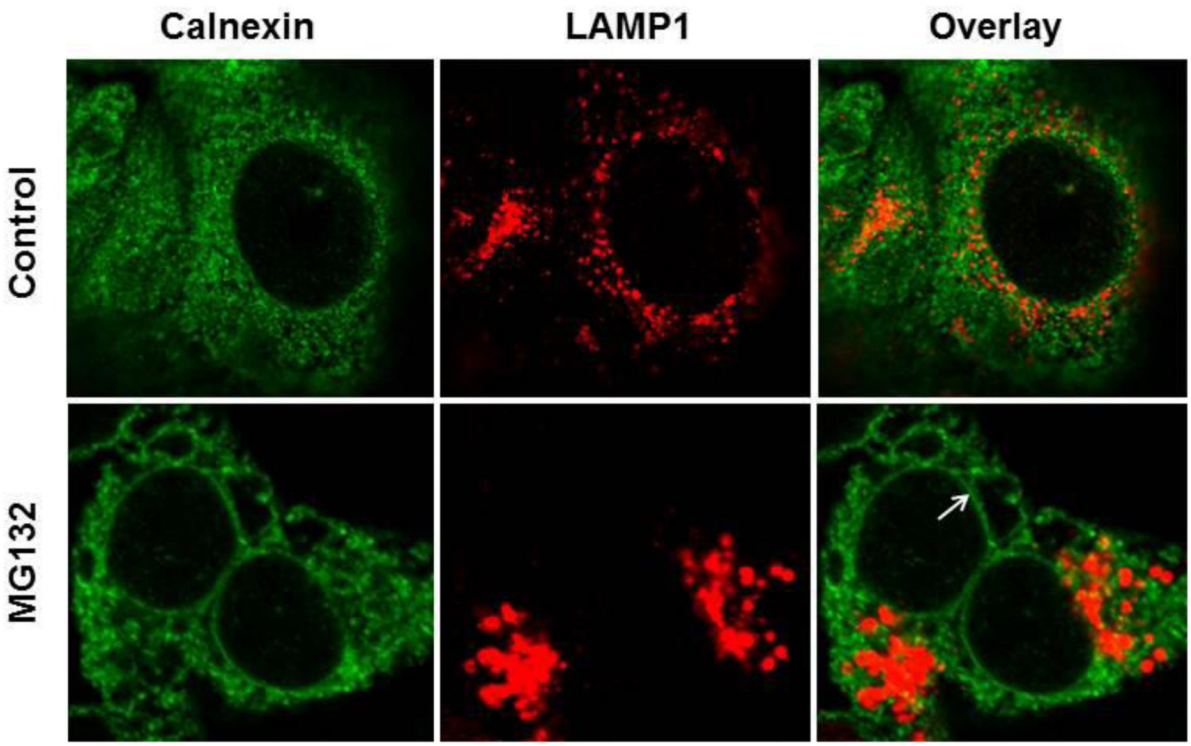

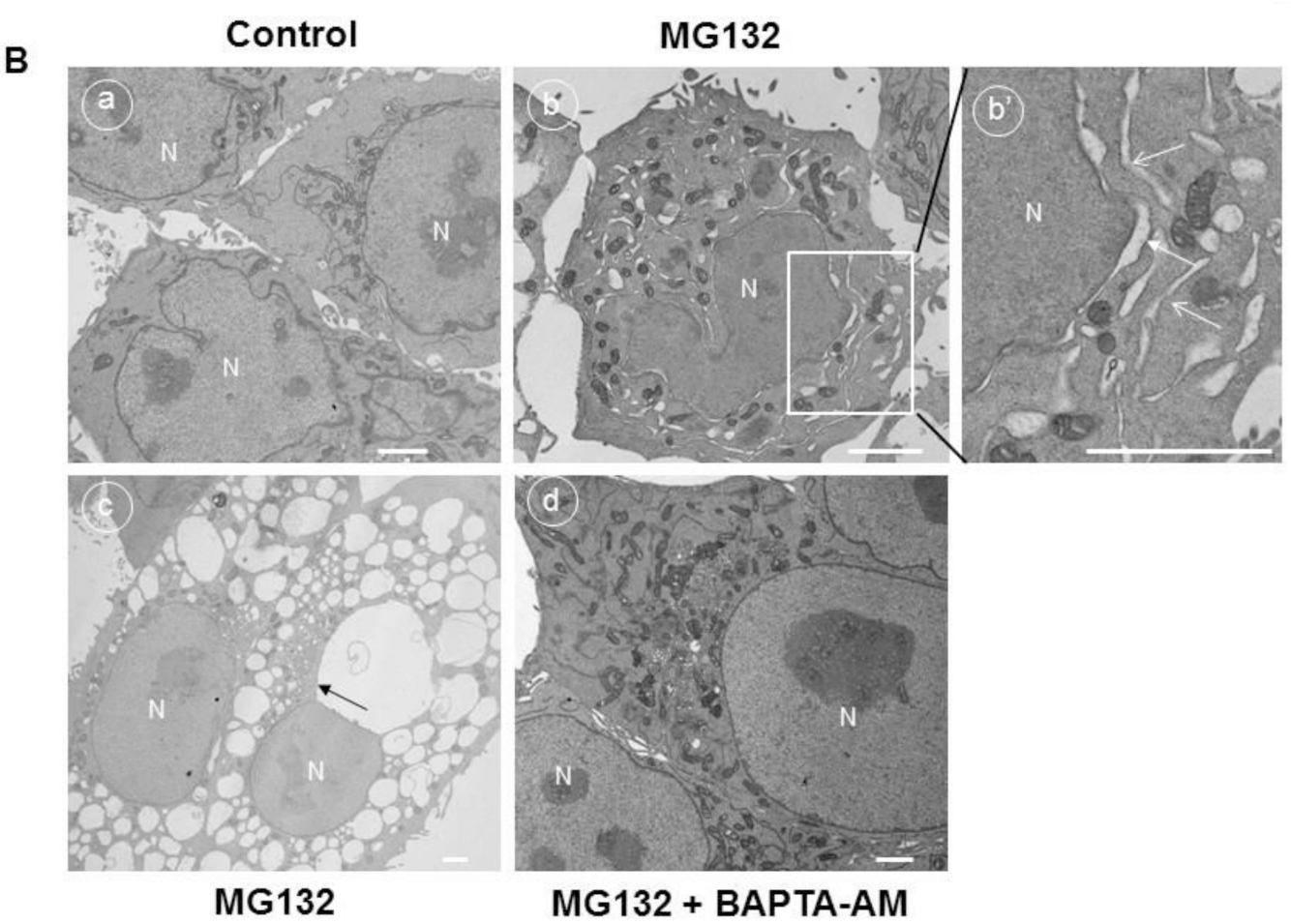

Figure 3. MG132 induced ER dilation in HCT116 cells

HCT116 Bax (−) cells were treated with MG132 (1 μM) for 16 hours, and cells were fixed with 4% PFA before immunostaining for Calnexin (green) and Lamp1 (red). Representative fluorescence images are presented in (**A**). (**B**) HCT116 Bax (−) cells were treated with MG132 (1 |μM) in the absence or presence of BAPTA-AM (10 μM) for 16 hours followed by Electron Microscopy. Panel a: untreated-control; panels b-c: MG132; panel d: MG132+BAPTA-AM. Panel b' is an enlarged photograph from the boxed area in panel b. N: nuclei, arrows: dilated ER. Bar: 500 nm.

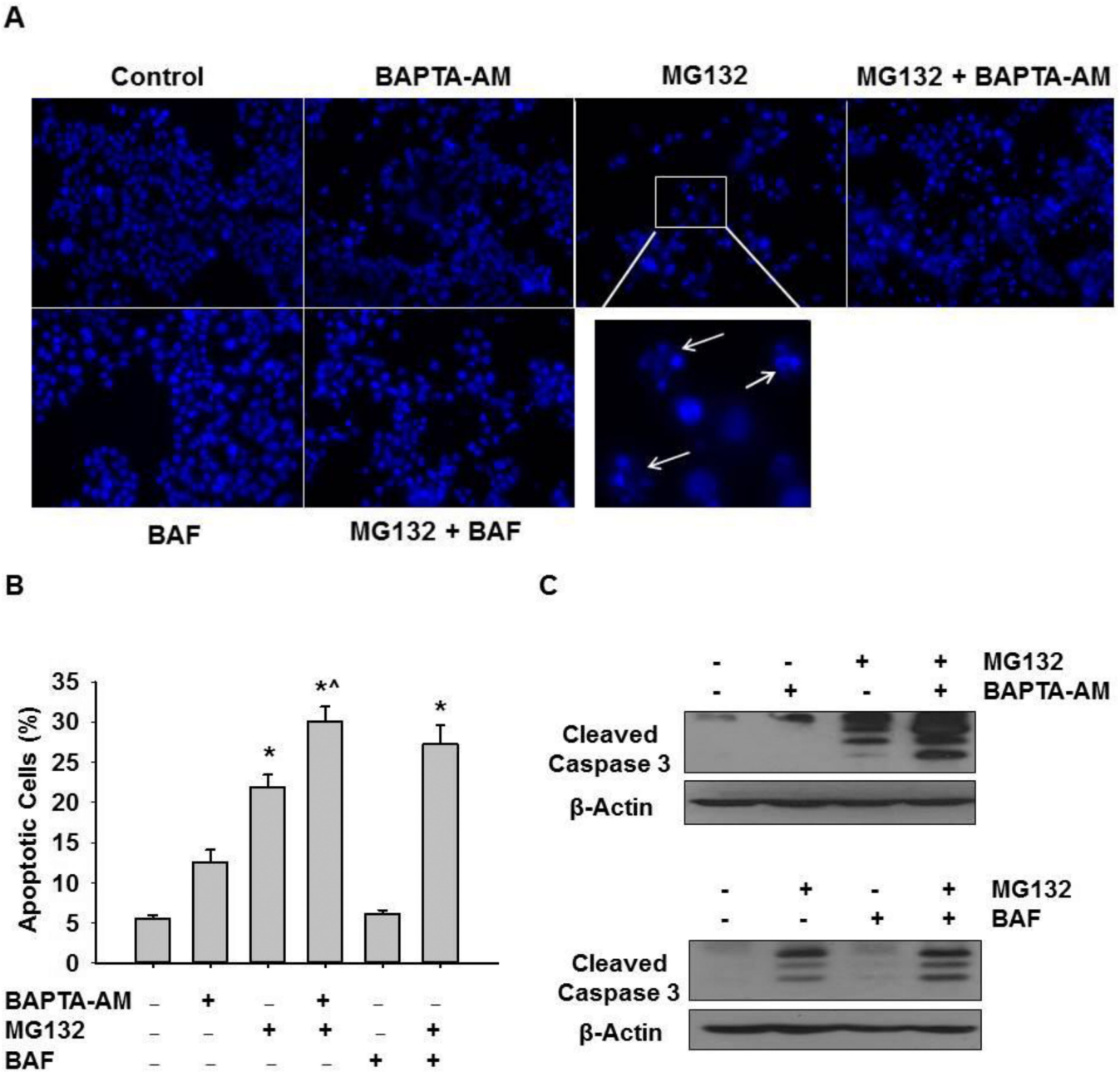

Figure 4. BAPTA-AM enhanced MG132-induced apoptosis

HCT116 Bax (+) cells were treated with MG132 (1 μM), BAPTA-AM (10 μM), and BAF (50 nM) for 20 hours before analysis of apoptotic cell death by Hoechst staining. Representative nuclear staining images are shown in (**A**). Apoptotic nuclei are demonstrated by chromatin condensation and fragmentation (arrows) as shown in the enlarged boxed area. (**B**) Apoptotic cells from Hoechst staining were counted, and results are represented by percent of apoptotic cells for each treatment (*$p<0.05$ vs untreated-control, ^ $p<0.05$ vs MG132, One Way ANOVA). (**C**) Cells were treated as described in 4A, and total lysates were subjected to western blot analysis for cleaved caspase-3.

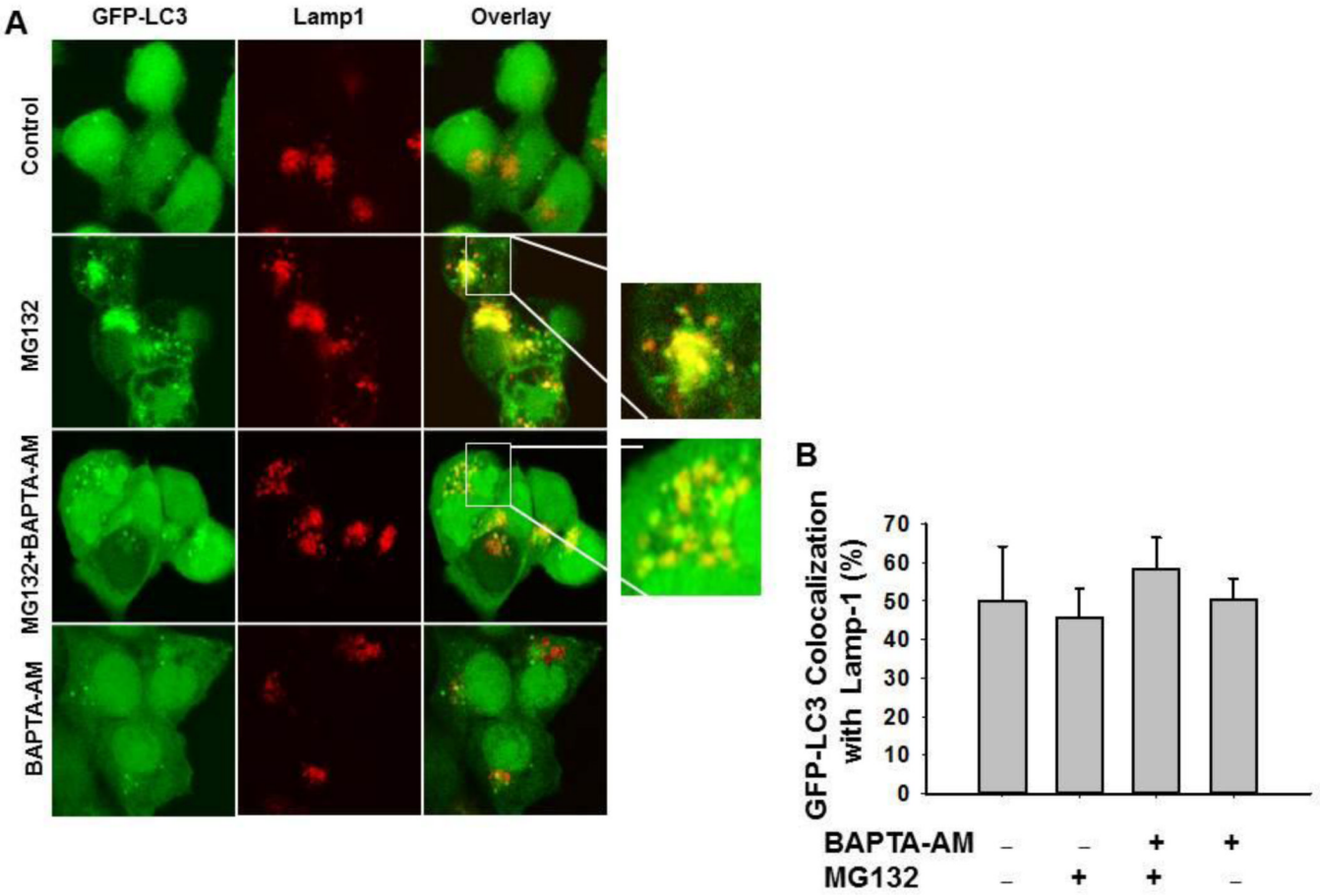

Figure 5. BAPTA-AM did not affect the colocalization of GFP-LC3 puncta with Lampl

Stable GFP-LC3 HCT116 Bax (−) cells were treated with MG132 (0.5 μM) in the presence or absence of BAPTA-AM (10 μM) for 20 hours. Cells were fixed with 4% PFA followed by immunostaining for Lampl and confocal microscopy. Representative fluorescence images are shown in (**A**). Right panels are enlarged photographs from the boxed areas indicating the colocalization of GFP-LC3 puncta with Lampl (**B**) The total number of GFP-LC3 puncta and the number of colocalized GFP-LC3 puncta with LAMP1 in each cell were quantified. At least 20 cells were quantified from each experiment, and data are presented as the percentage of colocalized GFP-LC3 with Lamp1 (Means ± SEM) from three independent experiments.

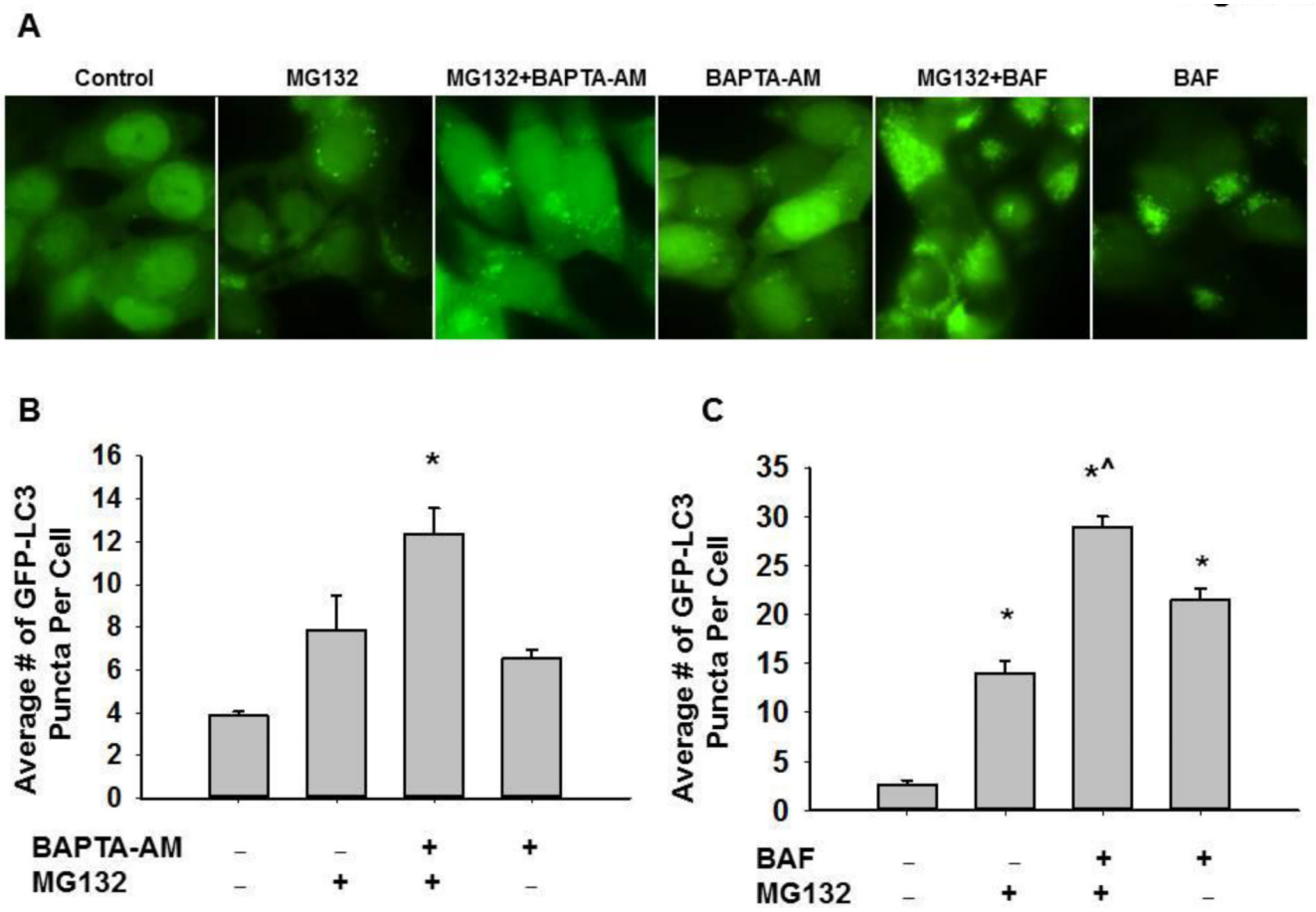

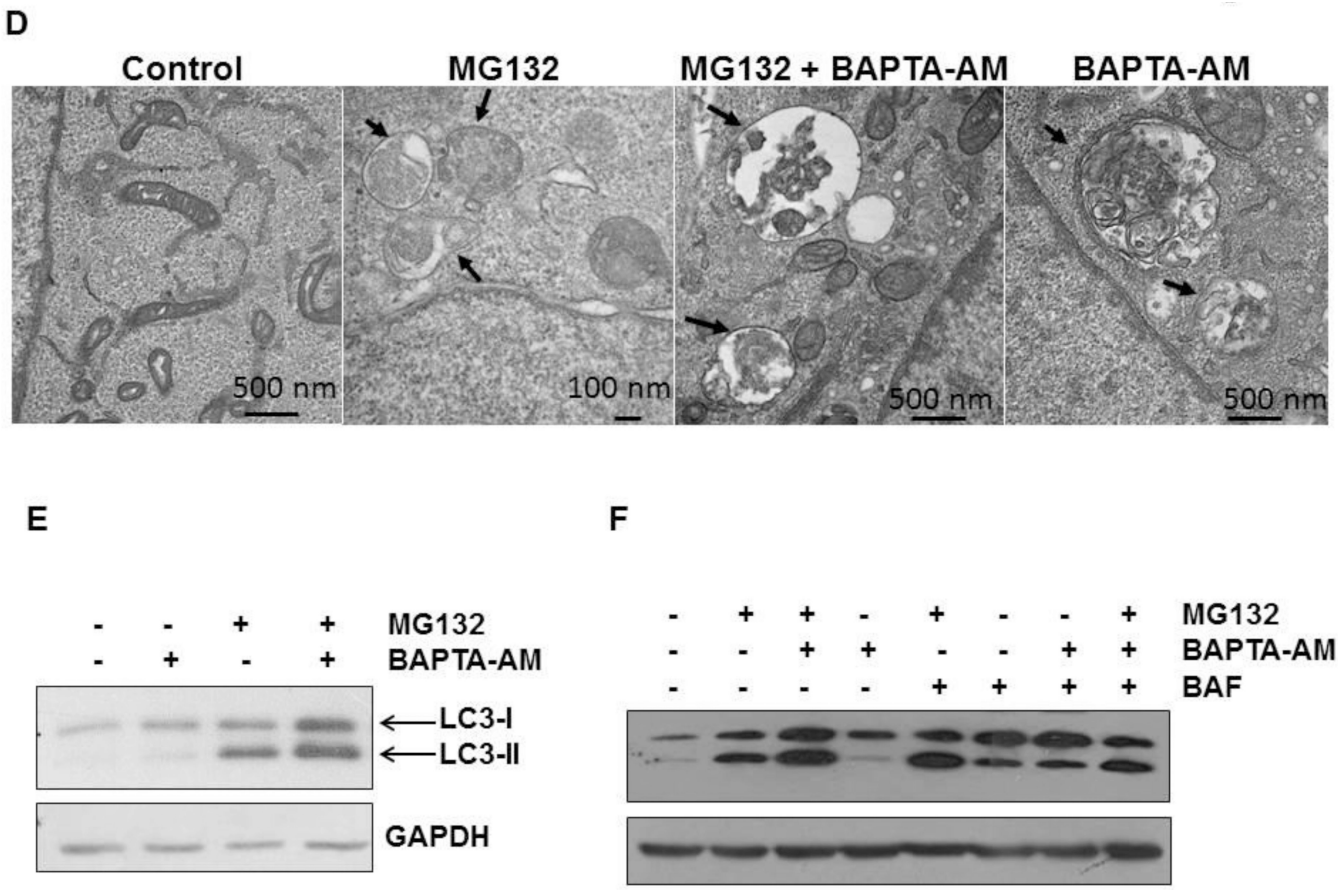

Figure 6. BAPTA-AM impaired MG132-induced autophagy

Stable GFP-LC3 HCT116 Bax (−) cells were treated with MG132 (0.5 μM) in the presence or absence of BAPTA-AM (10 μM) or BAF (50 nM) for 20 hours. Cells were fixed with 4% PFA followed by fluorescence microscopy. Representative fluorescence images are shown in (**A**). (**B and C**) The total number of GFP-LC3 puncta in each cell was quantified. At least 20 cells were quantified from each experiment, and data are presented as the average number of GFP-LC3 puncta per cell (Means ± SEM) from three independent experiments (*$p<0.05$ vs untreated-control, ^$p<0.05$ vs MG132, One Way ANOVA). (D) HCT116 Bax (−) cells were treated with MG132 (1 μM) in the presence or absence of BAPTA-AM (10 μM) for 20 hours. Cells were then processed for EM studies, and representative EM photographs are shown. Arrows: autophagosomes. (E) HCT116 Bax (−) cells were treated as in (D), and total cell lysates were subjected to western blot analysis. (F) HCT116 Bax (−) cells were treated with MG132 (1 μM), BAPTA-AM (10 μM), and BAF (50 nM) for 20 hours, and total cell lysates were subjected to western blot analysis.